

Evaluating S-Band Interference: Impact of Satellite Systems on Terrestrial Networks

Lingrui ZHANG^{*}, Zheng LI[†] and Sheng Yang[‡]

^{*} CentraleSupélec, Orange Innovation, email: lingrui.zhang@student-cs.fr

[†] Orange Innovation, email: zheng1.li@orange.com

[‡] CentraleSupélec, email: sheng.yang@l2s.centralesupelec.fr

Abstract—The co-existence of terrestrial and non-terrestrial networks (NTNs) is essential for achieving global coverage in sixth-generation cellular networks. Due to increasing spectrum demand, there is discussion in the world level to share some frequencies used in terrestrial Networks (TNs) with NTN, resulting in co-channel interference and performance degradation. This paper analyzes the interference caused by satellite networks on TN in the S-band. We examined the transmission mechanisms of satellite signals and conducted simulations to evaluate interference intensity across varying slant ranges. Our findings indicate that the angle between the user equipment direction and the sub-satellite point direction from the beam center significantly impacts the interference level.

Index Terms—Non-terrestrial network (NTN), terrestrial network (TN), low Earth orbit (LEO) satellite, interference, co-existence, data rate, spectrum sharing

I. INTRODUCTION

Non-terrestrial networks are expected to play a key role in sixth-generation (6G) cellular networks by enhancing coverage and connectivity in remote and underserved areas [1]. NTN includes various networks that operate through the sky, such as satellite networks, high-altitude platform systems (HAPS), and unmanned aerial vehicles (UAVs). In recent years, the significant decrease in satellite launch costs and the growing demand for global broadband have led LEO satellites to dominate NTN commercialization, with initiatives such as Starlink, OneWeb and AST SpaceMobile [2].

By integrating with TNs, NTNs can address coverage gaps, enhance infrastructure resilience during crises, and support high-bandwidth, low-latency applications like autonomous driving, crucial for the 6G era [3]. However, the deployment of NTN systems faces the challenge of limited spectrum resources. To address the limited bands and the small bandwidths of LEO satellite systems, there is indeed growing discussion about sharing TN bands with NTN systems [4], causing potential co-channel interference for TN users. As a terrestrial operator, understanding and managing interference between terrestrial and satellite networks is crucial. Therefore, it is essential to investigate the interference strength of a satellite to a TN user equipment (UE).

This paper provides an analysis of the interference caused by satellite networks on a TN in the S-band. The transmission mechanisms of satellite signals were studied through a literature review, forming the foundation for subsequent simulation and mathematical modeling. In the simulation, we analyze the

interference intensity of the satellite network in different slant ranges and find that with the beam center as the origin, the angle between the UE direction and the satellite direction has a significant effect on the interference intensity.

II. SYSTEM MODEL

The TN-NTN co-existence case studied in this paper is depicted in Fig. 1. In this case, a LEO satellite operates in

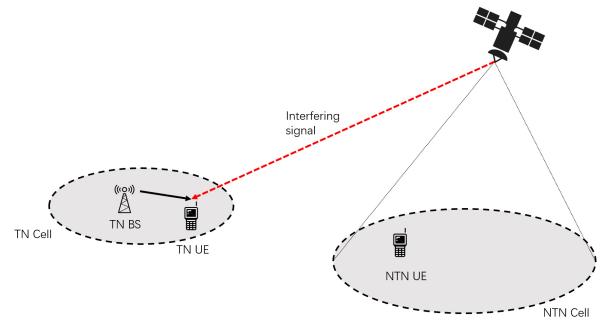


Figure 1. Co-existence scenarios

regenerative mode. The TN and LEO networks share the same frequency channels in the S-band. In this paper, we only focus on the downlink (DL) in the NTN and TN.

In the TN, the UE has an omnidirectional antenna type applicable to both TN and NTN connectivity. Only outdoor conditions are considered in this paper since building entry loss is so high that interference from satellites is negligible for indoor UEs [5]. Additionally, all UEs meet the flat fading criteria.

A. Space model

The space model is depicted in Fig. 2. Due to the significant distance between TN UEs and beam center of the NTN cell (up to hundreds of kilometers), the earth's curvature cannot be disregarded. In this scenario, the angle between the TN UE direction and the satellite antenna boresight direction is denoted by θ . We call this angle the misalignment angle. Furthermore, we define α as the angle between the UE direction and the sub-satellite point direction from the beam center. The distance between the UE and the satellite is denoted by d_u .

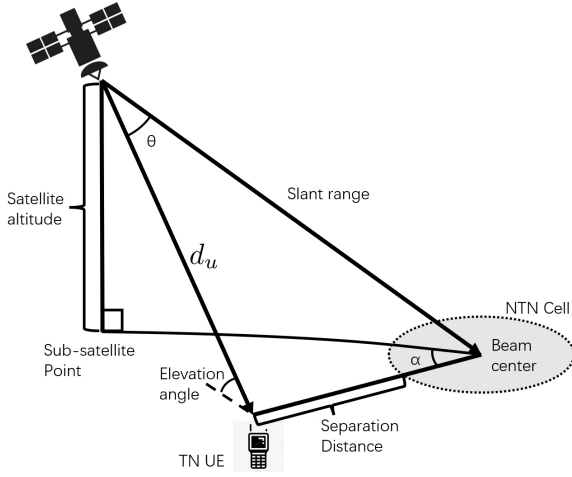


Figure 2. Space model

B. Satellite Signal Transmission Mechanism

In general, the received power (Rx power) per physical resource block (PRB) P_{Rx} can be expressed as follows:

$$P_{Rx} = \text{EIRP} + G(\theta)_{\text{dBi}} + \text{PL} + g + G_{Rx}, \quad (1)$$

where EIRP denotes the effective isotropic radiated power of the satellite, $G(\theta)_{\text{dBi}}$ represents the normalized antenna gain, PL indicates the path loss, g signifies the channel gain affected by small-scale fading, and G_{Rx} refers to the antenna gain of the UE [5]. All component are expressed in dB or dBi. In this paper, UE antenna gain is assumed to be 0 dBi.

Although specific antenna types vary, the following normalized antenna gain pattern $G(\theta)_{\text{dBi}}$, corresponding to a circular aperture theoretical antenna pattern, can be considered for satellite access network (SAN) parameterization and related coexistence studies [5]:

$$G(\theta)_{\text{dBi}} = \begin{cases} 1 & \text{for } \theta = 0^\circ, \\ 4 \left| \frac{J_1(ka \sin \theta)}{ka \sin \theta} \right|^2 & \text{for } 0 < |\theta| \leq 90^\circ, \end{cases} \quad (2)$$

In this equation, $J_1(x)$ represents the Bessel function of the first kind and first order with argument x . The parameter a corresponds to the radius of the antenna's circular aperture, while $k = \frac{2\pi f}{c}$ denotes the wave number. Furthermore, f denotes the frequency of operation, and c stands for the speed of light in a vacuum. The misalignment angle θ is measured from the bore sight of the antenna's main beam.

The signal path between a satellite and a terminal undergoes several stages of propagation and attenuation. The path loss (PL) is composed of the following components:

$$\text{PL} = \text{PL}_b + \text{PL}_g + \text{PL}_{c,r} + \text{PL}_s + \text{PL}_e, \quad (3)$$

where PL_b is the basic path loss, PL_g is the attenuation due to atmospheric gases, $\text{PL}_{c,r}$ is the attenuation due to rain and clouds, PL_s is the attenuation due to ionospheric or

tropospheric scintillation, and PL_e is the building entry loss [5]. All component are expressed in dB. The details to compute each part of the PL are omitted to conserve space.

The channel gain is computed by $g = |h|^2$ where h is the channel coefficient mainly influenced by small-scale fading. Specifically, the received signal is the sum of two components: the direct path signal and the diffuse multipath. The average direct path amplitude is considered to be normally distributed and the diffuse multipath component follows a Rayleigh distribution. Unlike path loss, g varies with time, and it can easily fall into a deep depression without line of sight (LOS). The duration of the deep depression and a good state (with LOS and slight shadowed fading) is described by a semi-Markov model. To obtain the channel coefficients, we need to set several parameters, such as carrier frequency, propagation environment type, elevation angle and Doppler shift correlation coefficient. The satellite speed, satellite elevation angle and UE speed should be considered constant during the simulation duration if limited by the small number of transmission time intervals (TTIs). Fortunately, we only consider the channel gains in the good state to estimate the maximum interference.

III. SIMULATION

In this section, interference analysis was conducted using MATLAB to validate the influence of interference signals over varying slant range. The separation distance shown in Fig. 2 is fixed at 100 km. The parameters for the system-level simulation are shown in Table I.

Table I
PARAMETERS FOR SATELLITE

Parameter	Unit	S-band
PRB size	kHz	180
Downlink frequency	GHz	2.17
Altitude	km	600
Antenna aperture (diameter)	m	0.44
Maximum antenna gain	dBi	40.4
Slant range	km	[600, 1075.19]
NTN Cell Diameter	km	45
Latitudes	degree	[-20, 20]
Elevation angle	degree	[20, 90]
Satellite peak EIRP per PRB	dBW	19.24
Earth radius	km	6378
TN signal-to-noise ratio (SNR)	dB	5.25
Channel gain	dB	-0.4

Figures 3 to 6 show the power on the transmitter side, the path loss and the received power on varying slant range. Figure 5 depicts the relationship between the received interference power and slant range for various angles α . Each curve except $\alpha = 90^\circ$ shows that the interference power initially increases with the slant range, reaches a peak, and then decreases. This is because the interference EIRP grows faster than the path loss in the first half, as shown in Fig. 3, while in the second half the path loss is more dominant. Moreover, lower angles ($\alpha = 0^\circ$ and $\alpha = 45^\circ$) result in higher peaks, indicating a lower path loss. Conversely, higher angles ($\alpha = 135^\circ$ and $\alpha = 180^\circ$) result in lower peaks and earlier occurrences due

to increased path loss, as shown in Fig. 4, and the fast decay increasing rate of antenna gain. This trend highlights the significant impact of the angle on interference power levels in satellite communication systems.

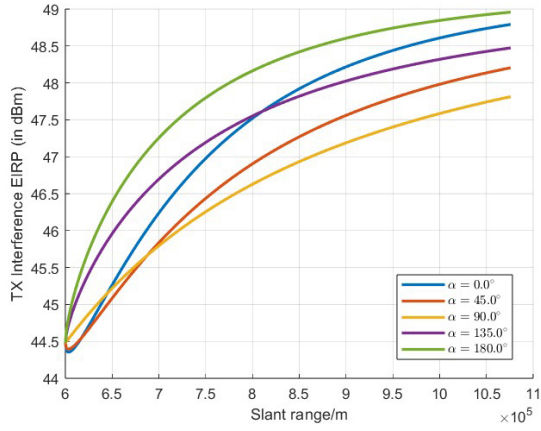


Figure 3. TX Interference EIRP on different slant range

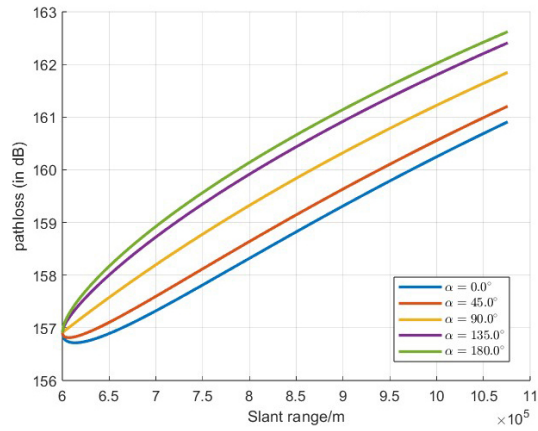


Figure 4. Path loss at varying slant ranges

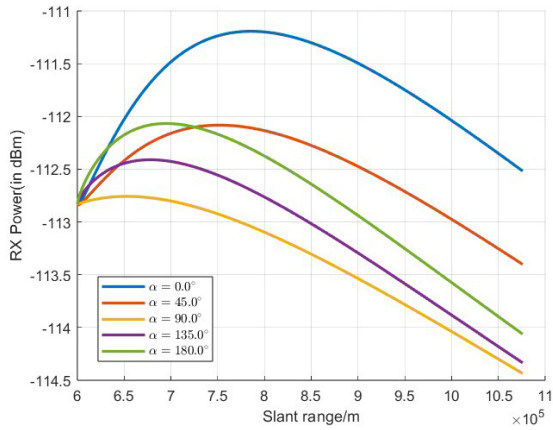


Figure 5. Received interference power per PRB on varying slant ranges

Figure 6 illustrates how the signal-to-interference-plus-noise ratio (SINR) changes with varying slant ranges for different

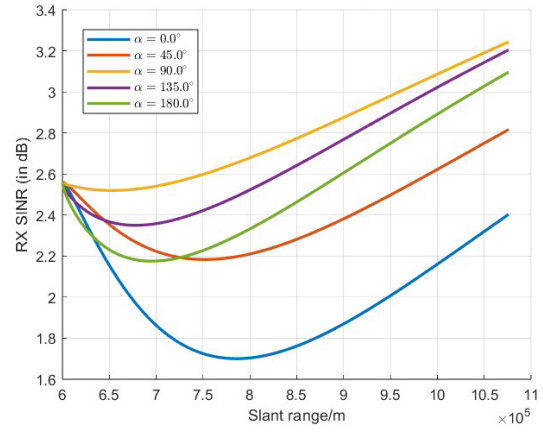


Figure 6. TN SINR on varying slant ranges (TN SNR=5.35 dB)

angles α . Despite a separation distance of up to 100 km, satellite interference still significantly reduces the SINR by approximately 2 to 4 dB. This impact remains significant and highlights the necessity of considering interference even with long separation distances in the TN-NTN co-existence case.

IV. CONCLUSION AND FUTURE WORK

In this paper, we investigated the mechanisms of satellite transmission and examined the variations in interference intensity across different slant ranges. Our findings indicate that the angle between the UE direction and the sub-satellite point direction significantly impacts the results with notable differences in RX power. Additionally, we observed the intriguing phenomenon of the SINR decreasing initially and then increasing with slant range. In our future research, we plan to analyze this issue from the perspective of separation distance to gain further insights.

REFERENCES

- [1] H. Xie, Y. Zhan, G. Zeng, and X. Pan, "LEO mega-constellations for 6G global coverage: Challenges and opportunities," *IEEE Access*, vol. 9, pp. 164 223–164 244, 2021.
- [2] X. Lin, S. Cioni, G. Charbit, N. Chuberre, S. Hellsten, and J.-F. Boutillon, "On the path to 6G: Embracing the next wave of low earth orbit satellite access," *IEEE Commun. Mag.*, vol. 59, no. 12, pp. 36–42, 2021.
- [3] M. M. Azari, S. Solanki, S. Chatzinotas, O. Kodheli, H. Sallouha, A. Colpaert, J. F. M. Montoya, S. Pollin, A. Haqiqatnejad, A. Mostaani, E. Lagunas, and B. Ottersten, "Evolution of non-terrestrial networks from 5G to 6G: A survey," *IEEE Commun. Surv. Tutorials*, vol. 24, no. 4, pp. 2633–2672, 2022.
- [4] S. Mahboob and L. Liu, "Revolutionizing future connectivity: A contemporary survey on AI-empowered satellite-based non-terrestrial networks in 6G," *IEEE Commun. Surv. Tutorials*, 2024.
- [5] "Study on New Radio (NR) to support non-terrestrial networks (release 15, v.15.4.0)," 3GPP, Sophia Antipolis, Valbonne, France, 3GPP Rep. TR 38.811, 2019.